Electronic Supplementary Information: Insights into the kinetics and self-assembly order of small-molecule organic semiconductor / quantum dot blends during blade coating.

Daniel T. W. Toolan*,[a] Michael P. Weir,[b,c] Shuangqing Wang,[c] Simon A. Dowland,[d] Zhilong Zhang,[e] James Xiao,[e] Jonathan Rawle,[f] Neil Greenham,[d] Richard H. Friend,[e] Akshay Rao,[e] Richard A. L. Jones[g] and Anthony J. Ryan[a]

[a] *Department of Chemistry, The University of Sheffield, Dainton Building, Brook Hill, Sheffield, S3 7HF, UK.*

[b] *School of Physics and Astronomy, The University of Nottingham, University Park, Nottingham, NG7 2RD, UK.*

[c] *Department of Physics and Astronomy, The University of Sheffield, Hicks Building, Hounsfield Road, Sheffield, S3 7RH, UK.*

[d] *Cambridge Photon Technology, J. J. Thomson Avenue, Cambridge, CB3 0HE, UK*

[e] *Cavendish Laboratory, Cambridge University, J. J. Thomson Avenue, Cambridge, CB3 0HE, UK.*

[f] *Diamond Light Source Ltd, Harwell Science & Innovation Campus, Didcot, Oxfordshire, OX11 0DE, UK*

[g] *John Owens Building, The University of Manchester, Oxford Road, Manchester M13 9PL, UK*

Experimental

Grazing Incidence X-ray Scattering Grazing incidence wide X-ray scattering (GIWAXS) was performed at I07 (Diamond Light Source, Rutherford, U.K.) at an X-ray beam energy of 12.4 keV. Scattering patterns were recorded on a vertically-offset Pilatus 2M detector with a sample to detector distance of 635.62 mm, calibrated using a silver behenate standard to achieve a Q range of 0.045 – 1.8 $Å^{-1}$. Alignment was performed via three iterative height (z) and rocking curve (Ω) scans, with the final grazing incidence angle set to Ω = 0.3º. The two-dimensional scattering patterns were masked to remove the sample horizon, detector module gaps and beam-stop and radially integrated from the apparent beam centre. Data correction and reduction was performed using the GIXSGUI MATLAB toolbox. [1] Two-dimensional scattering data was reduced to one-dimensional via radial integration, which was performed with a mask to remove contributions from “hot pixels”, the substrate horizon and reflected beam. Two-dimensional scattering data was reduced to one-dimensional via radial integration, which was

performed with a mask to remove contributions from “hot pixels”, substrate horizon and reflected beam. Fitting was performed using the *SasView* software package.[2]

In situ blade coating was performed using a home-made blade coater installed on the beamline (I07, Diamond Light Source) as pictured in Supplementary Figure 1. The blade was driven by a brushless DC motor [Premotech, BL48 EB (4 wire)], controlled via a National Instruments DAQ 621. The blade height was set via a micrometer built into the set-up. Approximately 100 µL of polymer solution was deposited via a syringe pump with a needle attached to the leading edge of the blade. Operation of the motor and the syringe pump was controlled and synchronised using LabView software.

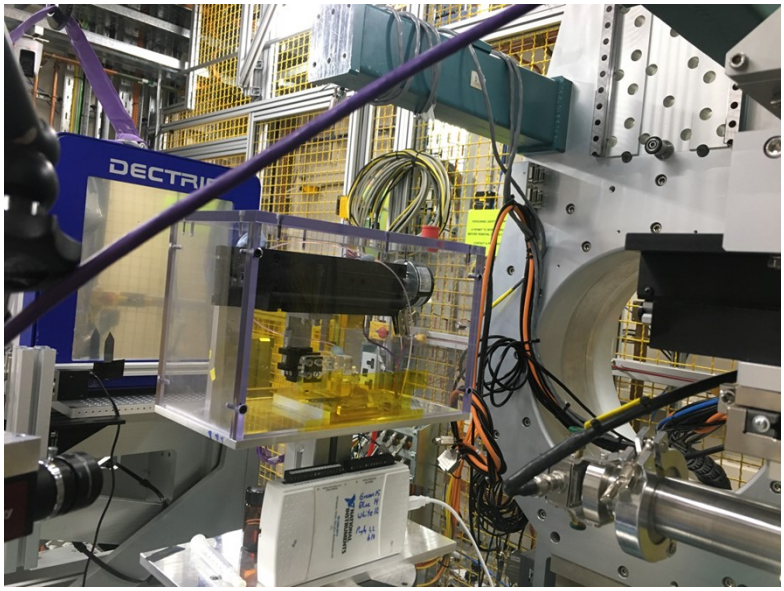

***Supplementary Figure 1**. Photograph showing the in situ blade coating set-up installed on the I07 beamline.*

Quantum dot synthesis and ligand exchange Synthesis of PbS quantum dots was carried out following the procedure by Hines and Scholes with modifications[7, 8] In summary, PbO (0.45 g), oleic acid (8 g) and 1-octadecene (10 g) were degassed in a three-necked flask at 110 °C for 2 h. The temperature was then reduced to 95 °C. Under nitrogen, a solution of bis(trimethylsilyl)sulphide (210 µL) in 1-octadecene (5 mL) was rapidly injected into the lead precursor solution. After cooling naturally to room temperature the PbS quantum dots were washed 4 times by precipitation/re-dispersion with acetone and hexane. The purified quantum dots were stored in a nitrogen filled glovebox at high concentration (>40 mg mL^{-1} / >100 µM) until use. Ligand exchange was carried out under nitrogen. The quantum dots in toluene were diluted to 8 mg mL^{-1} in a Toluene/THF mixture of 4:1. The ligand in 100 mg mL^{-1} THF solution was added to the quantum dot solution, keeping a ligand to quantum dot mass ratio of 1:1.

The ligand-exchanged quantum dots were then purified twice by precipitation and finally re-dispersed in toluene.

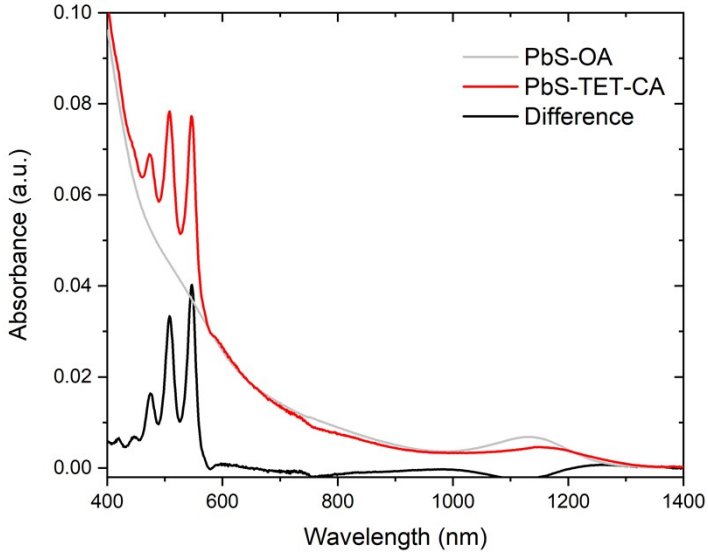

***Supplementary Figure 2**. Optical absorption spectra of PbS-OA, PbS-TET-CA after ligand exchange, and the difference (PbS-TET-CA – PbS-OA)*

Processing *in situ* scattering data

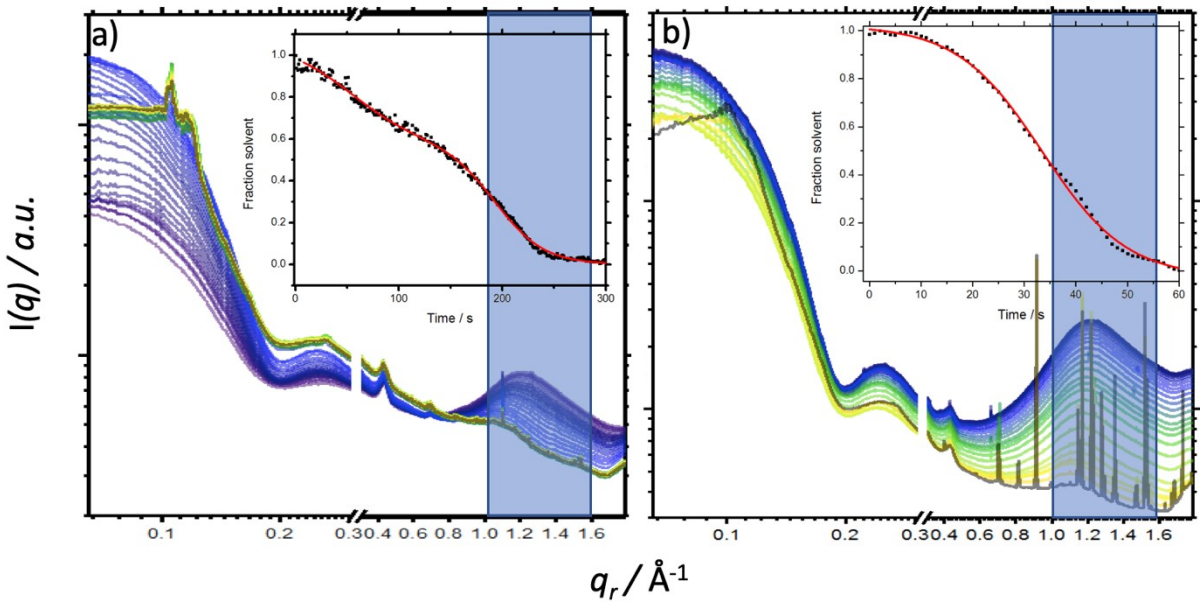

***Supplementary Figure 3**. Radially integrated scattering data showing q region employed to determine the effective solvent concentration (light blue box, q = 1.0 – 1.6 Å^{-1}), with insert showing the obtained fraction solvent as a function of time (black line) and corresponding fit (red line) for the TIPS-Tc:PbS-TET-CA (a) and TIPS-Ac:PbS-TET-CA (b) in situ blade coating series.*

Resampling in situ GIXS data. From the temporally resolved series of 1D radially integrated scattering data, the integral between q = 1.0 – 1.6 Å^{-1} was taken for each frame. Scattering in this region is extensively dominated by the toluene, thus, tracking the evolution of the "solvent peak" enables the estimation of an effective solvent fraction in the film. The resulting integrated scattering area as a function of time was normalised between one and zero, with one representing the fully solvated TIPS-Tc/TIPS-Ac:PbS-TET-CA solution and zero a fully dry TIPS-Tc/TIPS-Ac:PbS-TET-CA film, with data presented in Supplementary Figure 2a/b insert. This data was fitted to the following sigmoidal functions; $y = \frac{A_1 - A_2}{1 + e^{\frac{x - x_0}{dx}}} + A_2$, for the TIPS-Ac:PbS-TET-CA blend and, $y = A_1 + (A_2 - A_1)\frac{p}{1 + 10^{(LOGx01 - x)h1}} + \frac{1 - p}{1 + 10^{(LOGx02 - x)h2}}$ for the TIPS-Tc:PbS-TET-CA blend, with fit parameters given in Supplementary Table 1. From approach enabled the temporally resolved kinetic data series to be re-plotted, with respect to the effective solvent fraction, enabling both the 2D and 1D radially integrated scattering data to be sampled at effective solvent fractions from 1.0 to 0.0 at intervals of 0.01.

Supplementary Table 1.

	A1	A2	LOGx01	LOGx02	h1	h2	p
TIPS-Tc:PbS-TET-CA	5.56E-04	1.06275	53.31097	193.4051	-0.01325	-0.01832	0.45646
	A1	A2	x0	dx			
TIPS-Ac:PbS-TET-CA	1.02306	-0.02826	33.4562	8.18023			

Scattering

Sphere-hardsphere model In small-angle X-ray scattering (SAXS) of PbS nanocrystals suspended in an organic solvent such as toluene, the (organic) ligand shell and solvent are effectively contrast-matched and therefore scattering is dominated by the high electron density, metal-rich core. As PbS cores are quasi-spherical, they are adequately modelled as spherical scattering particles. The form factor of such particles, expressed as the scattering intensity as a function of the magnitude of the scattering vector, q, is given by

$$I(q) = \frac{scale}{V}\left[3V(\Delta\rho)\frac{\sin(qr) - qr\cos(qr)}{(qr)^3}\right]^2 + background$$

where r and V are the radius and volume of the sphere, $\Delta\rho$ is the scattering length density contrast difference between the solvent and the spherical particle. Whilst for conventional solution scattering data may be correctly normalised (i.e. at the experimental and initial data reduction stages) onto an absolute intensity scale in units of cm^{-1} the $scale$ represents the volume fraction of scattering particles. However, for grazing incidence scattering experiments it is not possible to normalise the scattering data onto an absolute intensity scale due to added complexities of the grazing incidence geometry. As such the scale, will be proportional to the volume fraction of scattering particles.

The expressions for $I(q)$ above are for isolated scattering objects, and are known as form factors since they describe the scattering features that emerge from the object's intrinsic shape and form alone. However, in a many-particle system like a solution or nanocomposite of colloidal quantum dots, scattering may also arise from inter-particle correlations. This scattering is taken into account by a ***structure factor*** $S(q)$ that multiplies the form factor at each point in q, i.e.

$$I(q) = F(q)S(q)$$

For relatively low concentrations of PbS colloidal quantum dots in an organic solvent, say 1-10 mg mL^{-1}, (as observed early in the drying process) the structure factor is a minor perturbation, such that it barely makes a visible adjustment to the data. If the system is sufficiently dilute it may be possible not to use the structure factor at all. In the *in situ* drying experiment here, as solvent is removed and the concentration of the quantum dots increases the structure factor becomes a significant feature of $I(q)$ and must be taken into account using the appropriate function. As the solvent volume fraction reduces further, the structure factor may begin to dominate the form factor such that correlations from inter-particle interactions are of primary importance in describing the observed scattering features.

The hard sphere structure factor (as implemented in *SasView* version 4.2.2) is a calculation of the interparticle structure factor for monodisperse spherical particles interacting through excluded volume interactions. This is calculated using the Percus-Yevick closure[3] where the inter-particle potential is given as:

$$U(r) = \begin{cases} \infty & r < 2R \\ 0 & r \geq 2R \end{cases}$$

The sphere hard sphere scattering model was employed to adequately fit the radially integrated scattering data for as deposited solutions (t = 0) of TIPS-Tc:PbS-TET-CA and TIPS-Ac:PbS-TET-CA with data presented in Supplementary Figure 6 and corresponding fit parameters in Supplementary Table 2.

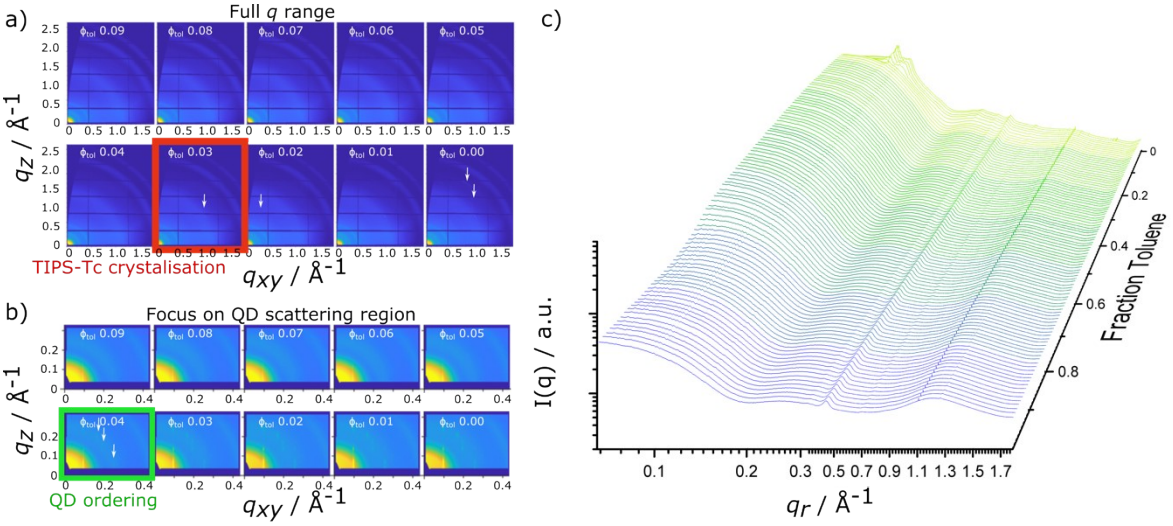

Supplementary Figure 4: *In situ* GIXS data for TIPS-Tc:PbS-TET-CA showing the latter stages of film-formation (0.09 > 0.00 volume fraction toluene), with (a) showing the full *q* range (QD + OSC lengthscales) and (b) focusing on the small angle *q* range (QD lengthscales). The TIPS-Tc and QD ordering is highlighted with red & green boxes and white arrows, respectively. Radially integrated *in situ* scattering data for **(c)** as a function of solvent fraction.

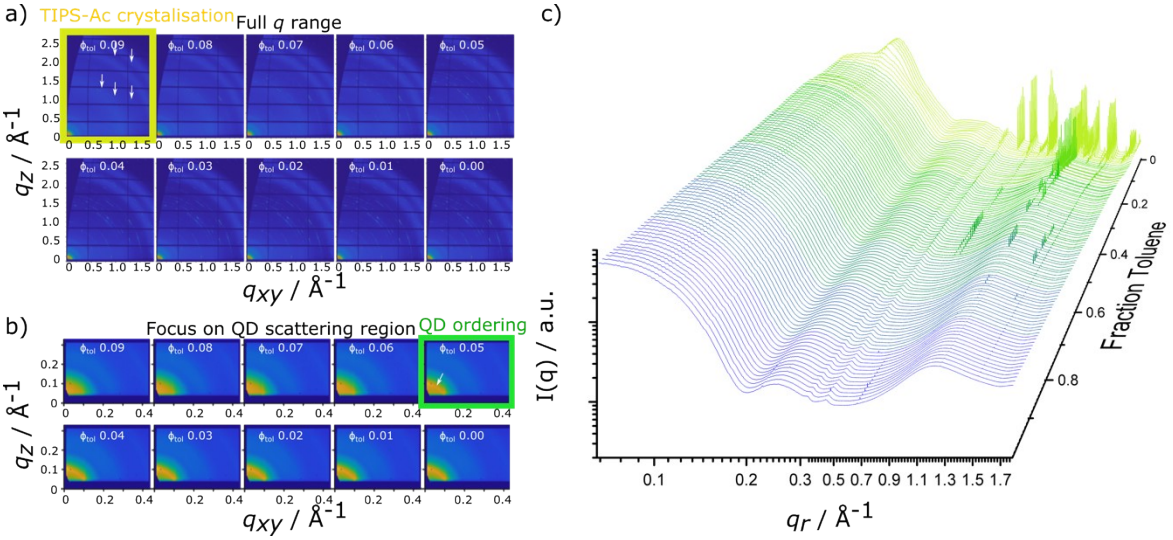

Supplementary Figure 5: *In situ* GIXS data for TIPS-Ac:PbS-TET-CA showing the latter stages of film-formation (0.09 > 0.00 volume fraction toluene), with (a) showing the full *q* range (QD + OSC lengthscales) and (b) focusing on the small angle *q* range (QD lengthscales). The TIPS-Ac and QD ordering is highlighted with yellow & green boxes and white arrows, respectively. Radially integrated *in situ* scattering data for **(c)** as a function of solvent fraction.

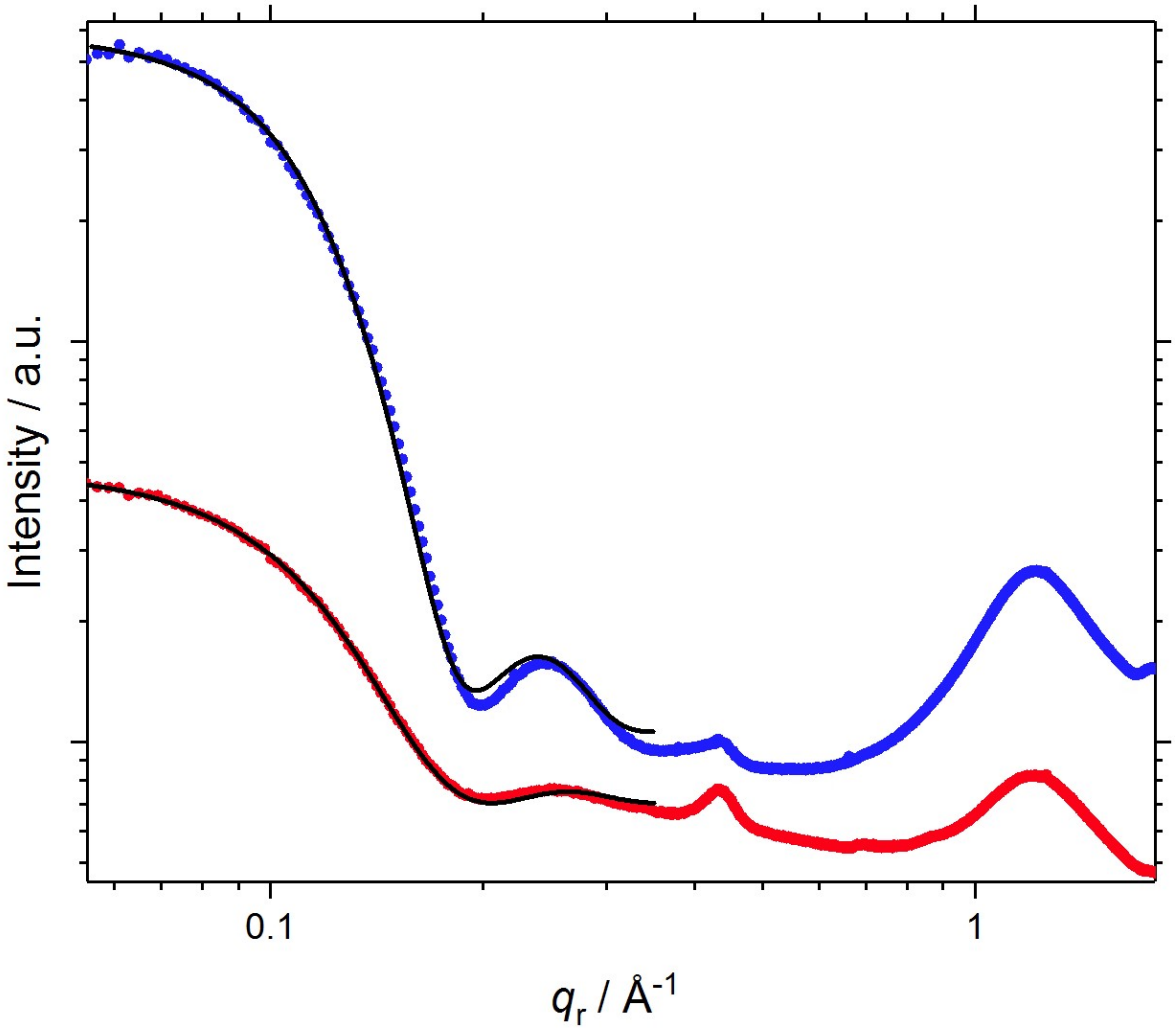

***Supplementary Figure 6**. Radially integrated grazing incidence scattering data for as deposited solutions (t = 0) of TIPS-Tc:PbS-TET-CA (red circles) and TIPS-Ac:PbS-TET-CA (blue circles), with fits from sphere*hard sphere model, respectively (black line).*

***Supplementary Table 2**. Fit parameters from sphere-hardsphere model, for as deposited solutions (t = 0) of TIPS-Tc:PbS-TET-CA and TIPS-Ac:PbS-TET-CA.*

	scale	Back-ground	Sphere SLD (10^{-6} Å^{-2})	Solvent SLD (10^{-6} Å^{-2})	Sphere Radius (Å)	radius.width	volfraction
TIPS-Tc:PbS-TET-CA	8.3812	706.99	50.7	10.2	22.847	0.1	0.11277
TIPS-Ac:PbS-TET-CA	142.39	973.9	50.7	10.2	22.847	0.1	0.087592

Face-centred cubic lattice with paracrystalline distortion The *sphere-hardsphere* model adequately describes the scattering from randomly ordered/dispersed quantum dots. However, as drying proceeds the experimental data presented here clearly shows the formation of scattering features commensurate with ordered quantum dot structures. Simulations presented in Figure 2 show that the quantum dots pack into an FCC type lattice.

The FCC paracrystal model (as implemented in *SasView* version 4.2.2) calculates the scattering from a face-centred cubic lattice with paracrystalline distortion. With the scattering intensity $I(q)$ calculated as:

$$I(q) = \frac{scale}{V_p} V_{lattice} F(q) Z(q) + background$$

where scale is the volume fraction of spheres, V_p is the volume of the primary particle, $V_{lattice}$ is a volume correction for the crystal structure, $F(q)$ is the form factor of the sphere (normalized), and $Z(q)$ is the paracrystalline structure factor for a face-centered cubic structure.

The lattice correction (the occupied volume of the lattice) for a face-centered cubic structure of particles of radius R and the nearest neighbour separation D is

$$V_{lattice} = \frac{16\pi}{3} \frac{R^3}{(D\sqrt{2})^3}$$

The distortion factor (one standard deviation) of the paracrystal is included in the calculation of $Z(q)$

$$\Delta a = gD$$

where g is a fractional distortion based on the nearest neighbour distance.

In order to better visualise the effect of the distortion factor on the ordering of quantum dots and their consequent ordering the “FCC paracrystal model” for 22.8 Å quantum dots is presented in Supplementary Figure 7, showing the case of highly ordered quantum dots with a low distortion factor and highly disordered quantum dots with a large value of the distortion factor. The corresponding pair distance distribution(Supplementary Figure 7 right) functions obtained from the simulated scattering data provide further insight regarding the distribution of the quantum dots depending upon the disorder of the FCC crystalline lattice.

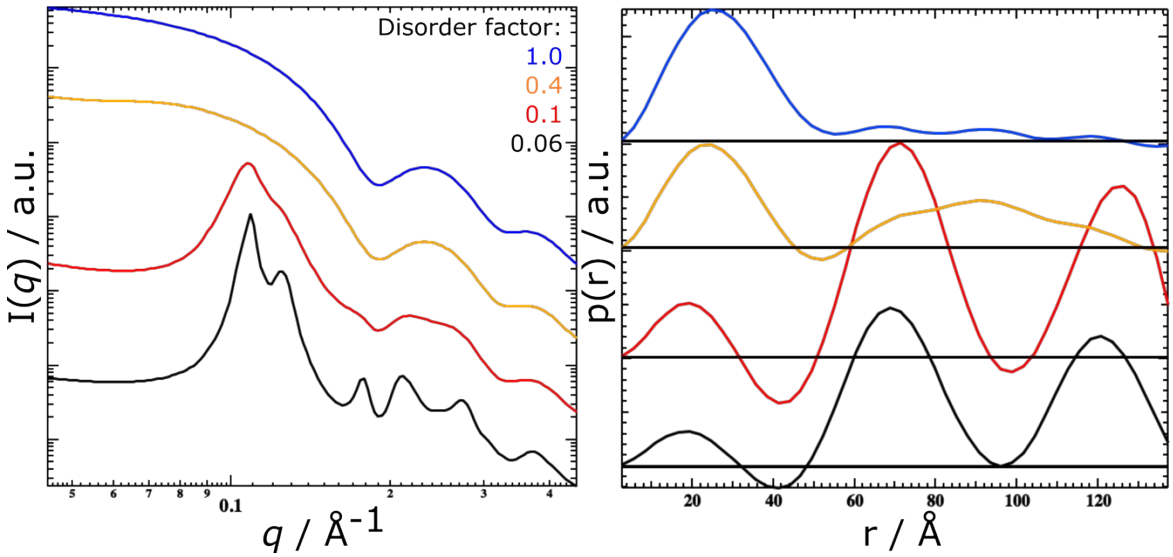

Supplementary Figure 7*. The effect of disorder factor on the packing of quantum dots using the FCC paracrystal model, were a) shows simulated 1D scattering data and b) shows pair distance distribution function obtained from the simulated scattering data.*

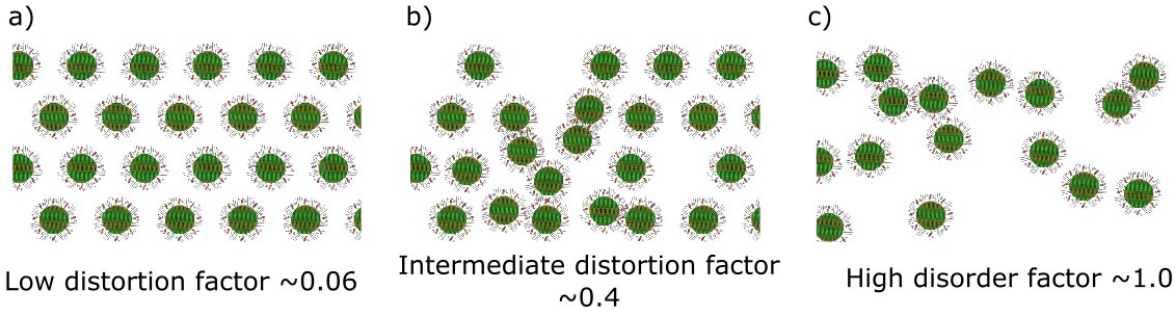

Supplementary Figure 8*. Illustration of effect of disorder factor on the packing of quantum dots using the FCC paracrystal model for low (a), intermediate (b) and high disorder (c) factors.*

For the *in situ* GIXS data presented here, the obtained scattering data could not be fitted to a single scattering model, as-such a combined model summing the dispersed (sphere*hard sphere) and ordered (FCC paracrystal) models was employed, where:

$$I(q) = F(q)S(q) + \frac{scale}{V_p}V_{lattice}F(q)Z(q) + background$$

Where $F(q)$ is the spherical form factor and $S(q)$ is the hard sphere structure factor.

Scattering fit parameters

Supplementary Table 3*. Fits parameters from sphere*hard sphere + FCC paracrystal model, for final cast films of TIPS-Tc:PbS-TET-CA and TIPS-Ac:PbS-TET-CA.*

	scale	back-ground	Sphere SLD (10^{-6} Å^{-2})	Solvent SLD (10^{-6} Å^{-2})	Sphere radius	Radius width	Sphere volfraction	FCC_scale	Lattice constant	d_factor
TIPS-Tc:PbS-TET-CA	4.820	927.35	50.7	10.3	22.847	0.1	0.15349	1.4639	102.66	0.06007
TIPS-Ac:PbS-TET-CA	100	600.07	50.7	10.3	22.847	0.1	0.00015	0.94466	99.034	0.16101

Author contributions

DTWT, MPW, SW, SAD and JR conducted scattering measurements. DTWT conducted model fitting, analysis and interpretation, and lead the writing of the manuscript. ZZ and JX synthesized QDs and performed QD ligand exchange. RALJ, AJR, AR, NCG and RHF conceived initial concept of the broader project as a whole. All authors contributed towards writing the manuscript.

References

1 Jiang, Z. GIXSGUI: a MATLAB toolbox for grazing-incidence X-ray scattering data visualization and reduction, and indexing of buried three-dimensional periodic nanostructured films. *J. Appl. Crystallogr.* **48**, 917-926, doi:10.1107/S1600576715004434 (2015).

2 Thampi, A. *et al.* Elucidation of excitation energy dependent correlated triplet pair formation pathways in an endothermic singlet fission system. *Journal of the American Chemical Society* **140**, 4613-4622 (2017).

3 Percus, J. K. & Yevick, G. J. Analysis of Classical Statistical Mechanics by Means of Collective Coordinates. *The Physical Review* **110**, 1 (1958).